Available online at www.sciencedirect.com
ScienceDirect
Current Opinion in Structural Biology

Coarse-grained models for protein aggregation

Chun Wu[1] and Joan-Emma Shea[1,2]

The aggregation of soluble proteins into fibrillar species is a complex process that spans many lengths and time scales, and that involves the formation of numerous on-pathway and off-pathway intermediate species. Despite this complexity, several elements underlying the aggregation process appear to be universal. The kinetics typically follows a nucleation-growth process, and proteins with very different sequences aggregate to form similar fibril structures, populating intermediates with sufficient structural similarity to bind to a common antibody. This review focuses on a computational approach that exploits the common features of aggregation to simplify or 'coarse-grain' the representation of the protein. We highlight recent developments in coarse-grained modeling and illustrate how these models have been able to shed new light into the mechanisms of protein aggregation and the nature of aggregation intermediates. The roles of aggregation prone conformations in the monomeric state and the influence of inherent β-sheet and aggregation propensities in modulating aggregation pathways are discussed.

Addresses
[1] Department of Chemistry and Biochemistry, University of California, Santa Barbara, CA 93106, United States
[2] Department of Physics, University of California, Santa Barbara, CA 93106, United States

Corresponding author: Shea, Joan-Emma (shea@chem.ucsb.edu)

Current Opinion in Structural Biology 2011, **21**:209–220

This review comes from a themed issue on
Theory and simulation
Edited by Jeffrey Skolnick and Richard Friesner

Available online 1st March 2011

0959-440X/$ – see front matter

DOI 10.1016/j.sbi.2011.02.002

Introduction

Protein aggregation involves the self-assembly of normally soluble proteins into large supramolecular structures. This process often results in disease either because the protein can no longer perform its function, or because of inherent toxicity of the aggregates. More than 20 such aggregation diseases have been identified, including Parkinson's disease, Alzheimer's disease and Type II diabetes [1,2]. Interestingly, several studies indicate that proteins not linked to any known disease can aggregate as well, provided conditions in which the native fold is destabilized and the solution is sufficiently concentrated [3,4]. The implication of these studies is that protein aggregation is an alternate pathway to folding, rather than necessarily an aberrant process. Indeed, in many organisms (including bacteria, fungi, invertebrates, and humans), protein aggregates serve a functional role [5]. Furthermore, fragments of proteins, as well as short *de novo* designed sequences can also aggregate, opening the door for using small aggregating peptides as building blocks for novel biomaterials [6].

The proteins involved in amyloid diseases are dissimilar, both in sequence and in native structure, yet electron microscopy (EM), X-ray diffraction and NMR studies indicate that the ordered end-products of aggregation are strikingly alike [7–10]. These fibrillar aggregates are composed of several protofilaments and typically range between 6 and 10 nm in diameter. They are highly enriched in β-sheet structure, with a characteristic 'cross-β' structure, involving β strands oriented perpendicular to the fibril axis [7,11–14]. Kinetic studies of aggregation point to a nucleation-growth process [15] (although more complicated scenarios have been proposed [16]). A lag phase is initially observed during which the nucleus for aggregation is formed, followed by a growth phase in which the nucleus rearranges and elongates to adopt a fibrillar structure. The lag can be eliminated by seeding the solution with a preformed nucleus. Experiments have revealed a variety of intermediate species present during the fibrillization process, ranging from small oligomers (as small as dimers), to soluble spherical aggregates, micellar species, amorphous aggregates, and protofibrils [17–21]. It is unclear whether these intermediates lie on-pathway or off-pathway to aggregation. It appears plausible that many different pathways, traversing different intermediate species, can be taken to reach a final aggregated state. Most aggregation intermediates are difficult to characterize experimentally (particularly the soluble species) as they correspond transient unstable species. Most of the available information on the structure of these oligomers has been of a low-resolution nature (mostly from AFM or EM pictures) [22–24], or provided indirectly by techniques that bulk average over several interconverting populations (CD or NMR measurements) [25,26]. Recent experimental advances in 2D-IR measurement [27] and ion mobility mass spectrometry [28,29], when coupled with fully atomic molecular dynamic simulations, are starting to provide atomically detailed structures of monomers and small oligomers. An emerging picture from these studies is the presence of a low population of β-rich conformations in the monomeric states of aggregating peptides such as Aβ and Islet Amyloid Polypeptide (IAPP) (peptides that are traditionally described as

natively unstructured). These states could serve as direct precursors for aggregation [29–33].

This short review focuses on the use of coarse-grained protein models to probe the aggregation process, with an emphasis on elucidating the pathways for fibril formation and identifying the nature of aggregation intermediates. Since protein aggregation appears to be a property of all polypeptide chains, and governed by fundamental interactions (such as hydrophobic and electrostatic) rather than by the details of the sequence, one can expect that simplified representations of the protein can yield powerful insights into the generic features of the aggregation process. We focus primarily on coarse-grained models published in the last two years. Excellent reviews have recently been published in COSB on fully atomic simulations of the early stages of aggregation [34] and of simulations of fibril structures [35], and we refer the reader to these articles.

Coarse-grained models for aggregation

As a result of the breadth in time scales (from ns for the formation of early oligomers to days, months and even years for the formation of mature fibrils) and length scales (from a nm sized protein to several hundred nm long aggregates) involved in aggregation, the computational study of this process lends itself to the use of a hierarchy of models. Different levels of resolution allow the probing of different elements of the aggregation process. Coarse-grained models, which possess simplified representations of the polypeptide chain, allow the extraction of general principles regarding the thermodynamics and kinetics of aggregation. Fully atomic models, on the other hand, can provide invaluable information at a detailed level not accessible to experiment, but they are restricting to probing the very early stages of aggregation [30,32,36–40] or the structural nature of preformed aggregates [41–43]. In contrast, the coarse-grained models that will be discussed in this review can easily handle hundreds of peptides and monitor the full aggregation process from monomer to fibril.

Coarse-grained models come in a number of resolutions, from models that represent the peptide as a single preformed unit [44,45•], to single bead lattice and off-lattice models [46,46,47••,48,49,50•,51], to multibead off-lattice models [52,53•,54••,55,56,57•,58,59••,60,61••,62,63•,64,65–68]. The dynamics of these models are propagated using Monte Carlo, Langevin and Discontinuous Molecular Dynamics, at times coupled with the use of enhanced sampling techniques such as replica exchange methods.

The parameterization of coarse-grained models can be done in a number of ways. Geometric quantities (bond lengths, bond angles, etc.) are typically obtained from structural data compiled in the Protein Data Bank (PDB). Energetic data (the strengths of the effective interaction potentials) are obtained either from knowledge-based potentials derived from a statistical analysis of the frequency of amino acid contacts in the PDB or from an energy gap optimization scheme [69–76]. The simplest bead models represent amino acids as either polar or hydrophobic, with hydrophobic–hydrophobic (H–H) pairs interacting via a Lennard–Jones potential. In these models, the energy contribution of an H–H contact is set so as to be consistent with free energies of transfer from nonpolar solvent to water for hydrophobic amino acids [77]. More sophisticated models, on the other hand, differentiate between different types of amino acids, with specific parameters for each of the twenty amino acids.

The models discussed in this paper are neither force-matched to reproduce all-atom simulations, nor are they parameterized to generate a given experimental aggregate structure nor a given aggregation mechanism. Validation of these models can be done in two manners: by comparison to fully atomic simulations, or by comparison to experiment. It is important to keep in mind that both forms of comparison have their limitations: fully atomic simulations are restricted to the very early stages of aggregation, while experimental measures of the aggregation process typically lack information about the structural nature of oligomers or mechanistic details of the aggregation process. In this review, we will highlight instances where the models show agreement with atomistic simulation and experiment. We emphasize that since the experiments generally lack atomistic information, and are themselves open to interpretation, the comparisons must remain at a qualitative level. The purpose of coarse-grained modeling is not only to 'agree' with experiment, but more importantly to offer new mechanistic insights, uncover the fundamental physical principles governing aggregation, and to offer testable predictions. A real strength of the coarse-grained models presented in this review lies in the fact that the parameters in the models can be varied so as to scan and explore a much larger parameter space than is typically accessible in experiment or atomistic simulation. As will be discussed below, this enables a study of how, for instance, the relative strength of the dihedral potential term (a measure of β-sheet propensity) can modulate the morphology of the aggregates and the aggregation pathway.

Figure 1 depicts the main models that will be discussed in this review.

Insights into the nucleation process

The precise nature of the aggregation nucleus is not known experimentally, primarily because the spectroscopic techniques employed (such as dynamic light scattering [78]) do not have the ability to follow the aggregation process with high spatial and temporal resolution. Several different

Figure 1

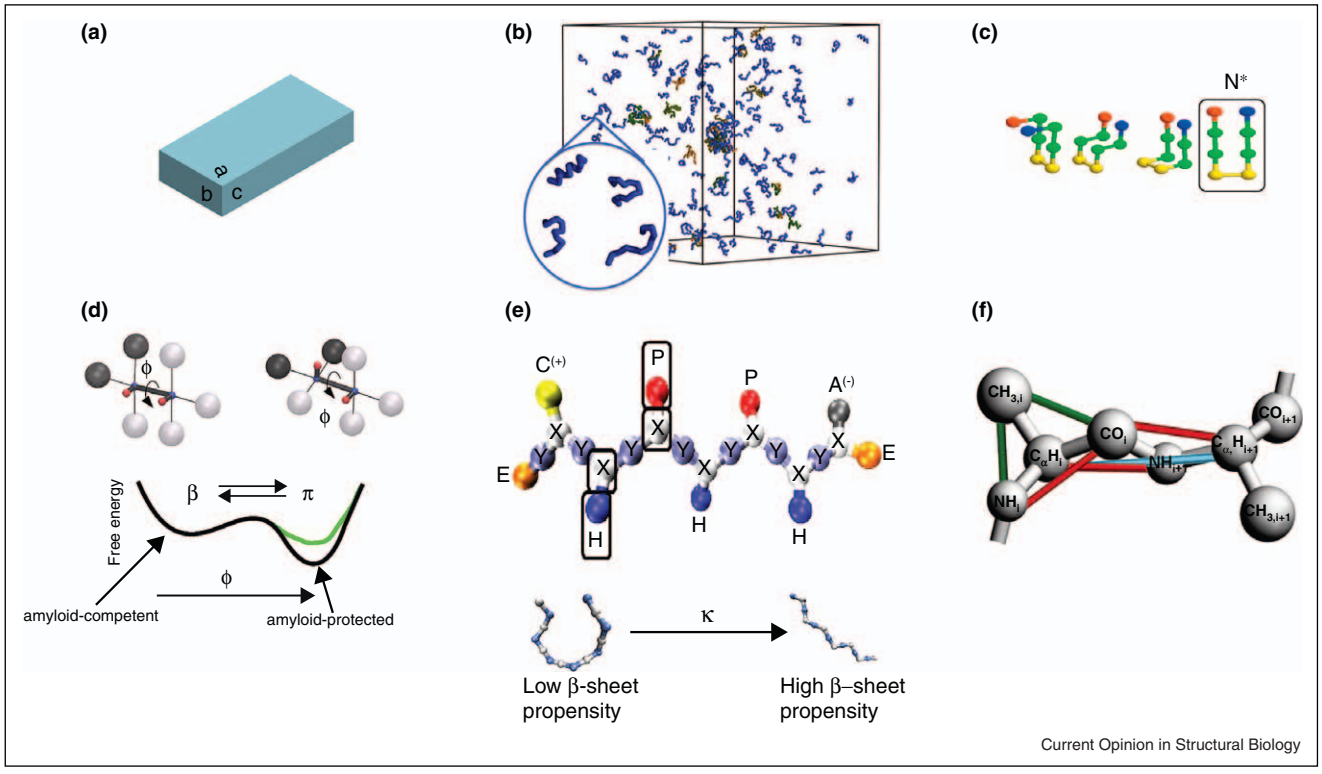

Main coarse-grained models discussed in this study. We note that higher resolution models exist that lie in between the coarse-grained models presented here and fully atomic simulations [125,126]. These models have enjoyed considerable success in modeling small oligomers, and are able to capture several detailed aspects of the sequence, but they do not yet allow (even with enhanced sampling) the simulation of aggregates larger than a few peptides. **(a)** Cuboid model. Adapted from [45•]. Each unit (which corresponds to an extended peptide, a folded peptide, or a small oligomer) is represented as a cuboid. Each unit is identical and conformational changes of the unit (for instance, ones that could occur upon binding) are not considered. The cuboid has three different interaction parameters, associated with the three pairs of surfaces (faces a–c), with strong attraction between cuboids in the intrasheet hydrogen-bonding direction, weaker in the intersheet direction, and repulsive in the direction parallel to the cuboid unit. Simulations are performed using a Monte Carlo procedure, with only single-unit moves considered. **(b)** Tube model. Adapted from [62]. Each peptide is represented by a flexible tube, with the position of each amino acid set by the coordinates of the C_α atom. The tube has a given thickness that accounts for excluded volume effects and a local bending stiffness. The peptide does not correspond to a particular sequence, but accounts for hydrophobic interactions through pairwise additive forces and for hydrogen bonding through geometric constraints. Simulations are performed using Monte Carlo or Discontinuous Molecular Dynamics. This figure illustrates an initial condition for simulation, involving a large number of peptides. The circle shows a zoom of different monomeric conformations populated. **(c)** Lattice model. Adapted from [47••]. Each chain consists of 8 connected beads on a cubic lattice, with sequence HHPPHH and charged termini. Different monomeric conformations are depicted. The N* denotes a fibril-competent structure that has already adopted a conformation similar to the one in the fibril. Simulations are performed using Monte Carlo simulations with local and global move sets. **(d)** Caflisch model. Adapted from [59••]. Each peptide unit consists of four spherical backbone beads and six spherical side-chain beads of hydrophobic and hydrophilic nature. Partial charges are present on the backbone to describe the backbone dipole. Each monomer interacts with other monomers via van der Waals and electrostatic interactions. The peptide has inherent flexibility that can be modulated through a dihedral term in the model such that the peptide populates to different extents: an amyloid-protected state π and an amyloid-competent state β. Simulations were performed using Langevin dynamics. **(e)** Shea model. Adapted from [54••]. The peptide geometry is a mid-resolution coarse-grained C_α–C_β model. The model peptide retains two interaction centers per residue (*X* and *Y*) along the backbone and one on the side chain. Four different types of side-chain groups are considered: *H*, *P*, *C* and *A*, where *H* stands for hydrophobic, *P* for polar, *C* for a positively charged cationic group, and *A* for a negatively charged anionic group. The peptide is capped on both sides by a capping group *E* (denoting end group). The sequence is chosen to have a binary core with the sequence *HPHPHP*, surrounded by two flanking oppositely charged residues (*C* and *A*) and two purely repulsive termini groups (*E*). Hydrogen-bonding and hydrophobic interactions are explicitly included. In addition, a dihedral term is present that determines the flexibility (β-sheet propensity) of the model. The atoms involved in this term are indicated by the rounded rectangles in the figure. Representative structures of the low and high β-sheet propensity structures are shown. **(f)** Hall model: [85]. The peptide is represented by an off-lattice model in which each residue consists of four spheres: three for the backbone (united atom NH, C_αH, and CO), and one for the side chain (denoted R). Backbone bond angles and C_α–C_α distances are enforced with pseudobonds. Simulations were performed using Discontinuous Molecular Dynamics, with all forces represented by hard-sphere (excluded volume terms) or square-well potentials (for hydrogen-bonding and hydrophobic interactions). Hall has recently developed a new version of PRIME that can describe all twenty amino acids [84].

nuclei have been proposed, including small-ordered β-sheet assemblies [27,79] and disordered micellar/globular type structures [20,25,78,80]. Simulations are uniquely poised to shed light into the nature of the nuclei, as well as into the nature of the species present during the lag phase.

Even very simplified models, such as those introduced by Pratko and Muthukumar [44,45•], can provide new insight into the nature of nucleation and lag phases. Using a cuboid model (see Figure 1a) Muthukumar [45•] and coworkers have identified two types of lag phases in aggregation. The first type, observed at high temperatures or low concentrations, corresponds to a classic nucleation mechanism, stochastic in nature and that can be seeded. The second type is observed at low temperatures and intermediate concentration and is due to slow Ostwald ripening. This type of lag phase is not affected by seeding. The simulations of Muthukumar lead to an important result: they suggest that nucleation is directly linked to the two-dimensional nature of fibrils (i.e. more than one β-sheet). Without direct intersheet interactions, nucleation is not present, and the growth curves do not show the characteristic nucleation-growth sigmoidal shape. Interestingly, Kashchiev and Auer [81] recently showed using classical nucleation theory that fibrils transform from a one-dimensional to two-dimensional aggregate in order to minimize formation work. Because of the simplified nature of the cuboid model, the simulations could not provide insight into whether or not the nuclei consisted of ordered or disordered species. The higher resolution models discussed below address these points.

The higher resolution 'tube' model of Auer and coworkers (Figure 1b) shows a clear condensation-ordering mechanism for aggregation [61••,62,63•,82]. The simulations [62,63•,82] show the initial formation of disordered, dynamic oligomers that are stabilized by hydrophobic and hydrogen-bonding interactions. Order emerges from this metastable state by the formation of small β-sheets that eventually align so as to form a cross-β structure. The underlying physical reason for the observed condensation-ordering mechanism is the existence of various metastable phases in the peptide phase diagram [64]. A direct calculation [62] of a nucleation barrier associated with this mechanism revealed a self-templated nucleation mechanism, with the surfaces of the β-sheets emerging from the disordered oligomers serving as templates for further fibrillar growth. Experiments on the prion protein have suggested just such a 'nucleated conversion model (NCC)' [83], with structurally fluid intermediates acting as initiation sites for fibril formation. The NCC was proposed to rationalize a number of experimental observations on the NM region of the Sup35 prion protein. This peptide is natively disordered, but adopts a β-rich fibril structure upon assembly. Sedimentation, light scattering and transmission electron microscopy were used to probe assembly; CD, Congo-red binding and limited proteolysis to probe structural changes and SDS solubility to probe stability. The combined experiments showed results that had elements, but were not fully consistent with either a pure templated assembly (TA) model or a pure nucleated-polymerization (NP) model. The TA model stipulates that an aggregated species is a template for the conversion of the soluble protein, and that this structural conversion is rate limiting. The NP mechanism, on the other hand, suggests that soluble monomers coexist with rarely populated monomers that have already adopted a fibril-competent conformation (N*) and that the rate-limiting step involves the association of N* conformations to form a critical nucleus for further aggregation. The experiments showed that structural conversion and assembly occurred simultaneously (in agreement with the TA model), but that the experimentally observed lag phase did not vary significantly with concentration, at odds with both the TA and NP models. Similarly at odds with the TA and NP models was the observation that assembly rates also did not vary much with concentration and that these rates reached a limiting value even in the presence of an excess of monomers. The assignment of oligomers consisting of 20–80 monomers (observed by scanning transmission electron microscopy) as 'on-pathway', offered an explanation of the aggregation kinetics and served as the basis of the NCC model. This model stipulates that ordered nuclei form within the micellar, unstructured oligomers, but the experiments do not provide information about precisely how this conformational conversion proceeds. The coarse-grained simulations of Auer are significant in providing direct mechanistic insight into how this nucleated conversion takes place. In the tube model, as in the ones that will be discussed below, seeding simulations supported a nucleation picture for aggregation by eliminating lag times.

The presence of disordered aggregates before fibril formation is corroborated by higher resolution models. In the simulations of Thirumalai and coworkers [47••] highly mobile oligomers are seen to form in the first stages of aggregation (a 'burst' phase). These oligomers coalesce in a second step to form a compact, but still disordered structure, with a significant amount of intra and inter-peptide contacts formed. As in the model of Auer and coworkers, β-structure begins to emerge within this large cluster. During this second step, the peptides undergo a conformational change to an aggregation prone state necessary for ordered assembly to proceed (N* in Figure 1c). The presence of disordered oligomers early in the aggregation process was also seen in the simulations of Hall and coworkers using the more sophisticated PRIME model (Figure 1f) [67,84,85]. Simulations of several polyalanine peptides, initiated from random dissociated states showed initial formation of small amorphous aggregates, which then coalesced into one large amorphous aggregate before forming β-sheet structure.

The structural nature of the early oligomers of a number of Alzheimer Amyloid-β (Aβ) protein alloforms and mutants were investigated by Urbanc and coworkers, using a model of the same flavor as Hall (Figure 1f), with residue-specific interactions [65,68,86]. These coarse-grained simulations were successful in reproducing differences in oligomer size distributions seen experimentally by PICUP/SDS–PAGE [87] and ion mobility mass spectrometry [28]. In addition, the simulations provided a structural characterization of the oligomers as well as the identification of the regions of the peptides involved in oligomerization, information that could be obtained from experiment alone. These simulations offer predictions regarding specific regions of the peptide that can be targeted to either enhance or prevent the oligomer formation.

It is well established experimentally that the cytotoxicity, aggregation propensity and aggregation pathways of a protein can be affected by mutation [88,89] or by changes in the experimental conditions [20,90,91]. In order to explore the role of this effect in determining aggregation pathways, Caflisch and coworkers [58,59••], and Shea and coworkers [52,53•,54••] introduced low-resolution to mid-resolution models in which the aggregation propensity of the peptide could be modulated. The model of Caflisch (Figure 1d) represents the peptide as a two-bead model which can populate two states: an amyloid-competent (β-stable) state and an amyloid-protected state (the β-unstable state). By modulating the relative stability of both states via a dihedral (flexibility) term, the authors observed different nucleation scenarios. For the β-unstable model, a classical lag followed by growth mechanism was observed. The lag phase was eliminated through seeding. The length of the lag phase was not constant in different simulations, highlighting the stochastic nature of the nucleation process. The formation of fibrils proceeded via the formation of micellar (nonordered β-structure) aggregates. Nucleation required either for several monomers already in a β-state to be close to each other within a single micelle, or for two micelles to interact so as to merge their β-subdomains. This is once again consistent with the experimentally observed NCC [83]. Interestingly, when the β-stable model is favored, nucleation corresponds to the direct assembly of monomers (already in the β-state) and does not involve the formation of micelles. Nucleation occurs at much lower concentrations for the β-stable model than the β-unstable model that requires concentrations above the critical micellar concentration. Shea and coworkers [52,53•, 54••] developed a three-bead model (two beads for the backbone and one for the side chain), with explicit hydrophobic and hydrogen-bonding interactions, coupled with Langevin dynamic simulations (Figure 1e). By varying a parameter related to a specific torsional degree of freedom, they modulated the flexibility of the peptide, in other words, its propensity to adopt a β-strand conformation in the monomeric state. Their simulations showed that for low β-sheet propensity, fibril formation proceeded through amorphous aggregates that internally rearranged into β-rich structures, consistent with the simulations of Caflisch and the NCC [83]. Intermediate levels of β-sheet propensity showed that fibril formation proceeded either through formation of amorphous aggregates, β-barrel (nonfibrillar) aggregates or directly from monomers into small β-sheet oligomers. At high β-sheet propensity, fibril formation proceeded uniquely through the formation of ordered aggregates, with initial formation of a single-β sheet, followed by the formation of a small double-layered sheet (the nucleus). The low aggregation propensity protein models of Shea and Caflish describe well several known aggregation proteins, such as the sup 35 prion protein that serves as the prototypical model of a protein undergoing a nucleated conversion process [83]. Mid-aggregation propensity proteins would correspond to the Alzheimer Aβ protein [28,92] or the IAPP protein [29] that populates a number of oligomeric species in the lag phase. Finally, high aggregating propensity models would emulate small aggregating fragments from larger proteins, such as the high-β sheet propensity phenylalanine-based peptides (the blocked charged termini FF [93] and KFFE peptides [94]), the GNNQQNY peptide from sup 35 [95] and certain functional amyloid proteins [5], all of which do not appear to have on-pathway disordered intermediates.

The role of β-sheet propensity in aggregation has been studied experimentally by Tjernberg *et al.* [94], who showed that peptides with high β-sheet propensity (such as KFFE) formed fibrils while similar peptides with low β-sheet propensity (such as KAAE) did not form ordered aggregates. These findings are in line with the predictions from the coarse-grained simulations described above. Furthermore, fully atomic simulations of the KFFE and KAAE peptides [96,97] show that KFFE formed more stable, β-rich dimers than KAAE. Another example of how the extent of β-structure in the monomeric state dictates aggregation, as predicted by the Shea and Caflisch models, can be found in recent ion mobility mass spectrometry, 2D-IR and fully atomic simulation studies of the IAPP [29,98,99]. IAPP exists in two forms, a human form that can aggregate to form fibrils, and a rat form that differs only by 6 amino acids but that cannot fibrillize. Combined experimental and computational studies show that the human form populates β-rich conformations in the monomeric state [29] and dimeric state, while the rat form does not.

Modulating the aggregation propensity of the model is another way of modulating the experimental conditions: in this respect, tuning the aggregation propensity of the Caflisch and Shea models can reflect tuning the pH of the solution. Experiments by Dobson [20] show that slight changes in the pH can change the aggregation pathway

from one populating disordered intermediate, to one populating ordered protofibrillar species, much as seen when the β propensity is altered in the coarse-grained models. Adding fluorinated alcohol to a solution of the Aβ(1–42) peptide as was done in the experiments of Picone and coworkers [90] can shift the population to a 'β-unstable' helix state, preventing the formation of β-rich oligomers.

The works of Caflisch and coworkers and Shea and coworkers lead to the prediction that peptides with lower β-sheet propensities lead to a greater number of prefibrillar species. Since toxicity is being increasingly linked with prefibrillar entities rather than full-fledged fibrils, it is tempting to speculate that peptides with higher β sheet propensities form 'less toxic' aggregates than those formed by peptides with lower β sheet propensities. These simulation results could explain why certain mutants that decrease β-sheet propensity (such as the E22G Arctic mutant of the Alzheimer Amyloid-β protein) lead to enhanced oligomer formation over the wild-type species [100,101].

Insights into the growth process

The growth phase corresponds to the conversion of the nucleus into a full-fledged fibril. Transient intermediates known as protofibrils have been observed before the presence of fibrils and these species have been reported as possible direct precursors to fibrils [102]. Protofibrils share many of the characteristics of fibrils, but are smaller, more flexible and less ordered. They bind to ThT and exhibit protection from hydrogen–deuterium exchange, but to a lesser extent than full-fledged fibrils [103,104]. They possess cross-β core structure and come in a variety of shapes, from pore-like, to spherical, to extended filaments [101,104]. The mechanisms by which the nucleus transforms into protofibrils, how protofibrils transform into fibrils, and how the fibrils further grow into larger structures remains poorly understood. Kinetic studies based on light scattering and AFM studies suggest that protofibrils can grow laterally by protofibril–protofibril assembly and longitudinally by monomer addition. The fibrils themselves can grow lateral and longitudinally [105–108]. On the basis of an analysis of kinetic experiments on the deposition of monomers onto fibrils, Straub and coworkers proposed a theoretical framework for monomer deposition and resulting fibril elongation consistent with experiment [109,110]. They suggested two possible mechanisms: firstly, the formation of an amyloid-competent monomeric conformer (i.e. N*, a conformation that has already adopted the conformation of the peptide in the context of the fibril [31,111]) that deposits on the fibril and secondly, a 'dock-lock' mechanism (similar to the one suggested by the experiments of Maggio [112,113]) in which the monomeric peptide first adsorbs onto the fibril (the 'dock' phase) and then undergoes a structural rearrangement to adopt a conformation commensurate with the fibril structure ('lock' phase). Other experimental studies of fibril formation point to a mechanism by which fibrils grow from micelles that convert to fibril nuclei once they have reached a critical size [78], or directly from oligomers [114] that first grow laterally to full fibril thickness (a distinct mechanism from lateral protofibril assembly) and in a second step grow longitudinally into fibrils.

The coarse-grained simulations described in the next few paragraph provide important new mechanistic information regarding the growth phase that complement experimental observations.

The cuboid simulations of Muthukumar and coworkers [45•] show that the fibril is in dynamic equilibrium with the peptides in solution and that fibril growth is not uniform. Their simulations indicate that fibril growth proceeds via an 'Ostwald ripening' mechanism, in which smaller fibrils 'lose' peptides to larger fibrils via a diffusion process (in other words, the larger objects grown at the expense of the smaller ones). These simulations are consistent with earlier lattice simulations by Thirumalai [47••] that showed that this Ostwald ripening mechanism quantitatively follows the Lifshitz–Syazov growth law. The simulations indicate that the protofibrils can play two roles: they can serve as on-pathway precursors to full-fledged fibrils, or as off-pathway monomer reservoirs. This is an important result, as it reconciles much experimental debate about the role of protofibrils [18,105]. Fibril growth was seen to be hindered at very high temperatures due to the high diffusion of the monomers (and hence high likelihood of desorbing from the fibril).

The higher resolution models provide more detailed insights into the fibril elongation phase. In the simulations of Hall and coworkers [67,84,85], fibril growth occurs in two ways that are consistent with experimental observations: by lateral addition of β-sheet layers, and by β-sheet elongation by the addition of monomers at the extremities of the fibril. Both modes are equally represented in the early phases of fibril growth, but the β-elongation mode dominates in the later phases. The mechanism of longitudinal growth by monomer addition and lateral growth by 'templated protofilament assembly', was also observed in the off-lattice simulations of Auer, Caflisch, and Shea [52,53•,54••,58,59••,81]. These simulations support the two main monomer-addition elongation mechanisms suggested by Straub. Using a Markov Chain approach, Calfisch and coworkers investigated the efficiency of the dock-lock mechanism and found that the dock-lock mechanism was the dominant elongation mechanism at play both for the β-stable model and for the β-unstable model.

An analysis of the role of β-sheet and aggregation propensity reveals that the number and heterogeneity of pathways to fibril formation increase with decreasing

β-sheet (or aggregation) propensity. Peptides with low β-sheet (aggregation) propensities can populate on-pathway and off-pathway intermediates to fibril formation, while peptides with high β-sheet (aggregation) propensities tend to assemble directly from ordered oligomers into fibrils, without populating off-pathway intermediates. While both peptides with high and low β-sheet (aggregation) propensities can grow via lateral addition, they do so in different ways: peptides with high β-sheet (aggregation) propensity tend to grow by the addition of a preformed sheet that adds on to the existing fibril, while peptides with low β-sheet (aggregation) propensity tend to grow from an assembly of disordered, deposited monomers that rearrange their structure on the surface of the fibril. The models with high β-sheet propensity populate N* (fibril-prone) conformations to a larger extent than the low β-sheet propensity conformations. In recent simulations, Thirumalai and coworkers investigated the role of aggregation prone conformations (N* in Figure 1c) in determining the rate of fibril formation [50•]. Their simulations predict that enhancing the population of fibril-prone conformations in the monomeric state via mutagenesis or chemical means would increase the rate of fibril formation [50•]. This prediction was confirmed both in all-atom simulations [33] and in the experiment by Meredith and coworkers where the chemical cross-linking of the D23 and K28 residues in the $A\beta_{1-40}$ peptide enforced a fibril-like conformation in the monomeric state and enhanced the rate of fibril formation [115].

In addition, coarse-grained simulations show, in agreement with experiment, that the aggregation pathways and end-product of aggregation differ depending on the experimental conditions (such as temperature and concentration), or the nature of the peptide. Peptides with low β-sheet propensities can have as final states amorphous aggregates and β-barrels (as well as fibrils), while peptides with higher β-sheet propensities populate fibrils (and to a lesser extent 'off-pathway' β-barrels). Experimental confirmation for these predictions can be found in the experiments of Tjernberg *et al.* [94] in which peptides with high-β sheet propensity (such as KFFE) formed fibrils, while those with low (such as KAAE) did not form ordered aggregates. The effect of temperature and concentration on aggregation was explored in a number of coarse-grained models. In the simulations of Hall, at low temperature, the aggregates tend to be amorphous or nonfibrillar and the system is kinetically trapped. Fibrillization is favored at high temperatures and concentration, although fibril formation is seen to decrease after a certain critical temperature. The simulations of Auer *et al.* [82] show that at low concentrations the formation of fibrillar structures does not proceed via the formation of disordered oligomeric precursors, but rather the polypeptide chains convert directly into β-sheet structures. With increasing concentrations, the formation of disordered oligomers becomes increasingly favorable, but their structural properties are temperature dependent. Below their unfolding temperature, individual polypeptide chains within the oligomers remain substantially folded. By contrast, with increasing temperatures, the fraction of unfolded polypeptide chains increases, and the oligomers become more disordered. Muthukumar and coworkers found that while increasing temperature leads to longer (and fewer) fibrils, too high temperatures lead to fibril disassembly, so that a non-monotonic dependence on fibril size and on total number of fibrils with temperature was observed. It is well known that the morphology of fibrils is exquisitely sensitive to preparation conditions, with slight changes in mechanical agitation leading to fibrils of different appearances [116]. Caflisch and coworkers [60] examined the polymorphism of fibrils resulting from their simulations and found the origin of the polymorphism to be of kinetic nature, with different fibril morphologies having different oligomeric intermediates (from micelles to protofibrils). Lattice simulations suggest that this polymorphism may already be encoded at the monomeric level, with different N* structures dictating different fibril morphologies [50•].

Emerging areas

Emerging areas of research, topics that once again are better served with coarse-grained models rather than fully atomic ones, involve the incorporation of elements of the 'cellular milieu' into aggregation. One important, and still incompletely understood area is the effect of crowding on aggregation. Caflisch and coworkers [57•] have begun such an investigation and their simulations indicate that the effect of crowders differs for peptides with high aggregation propensity and for peptides with lower aggregation propensity. In the case of the peptides with low aggregation propensity, the rate-limiting step is the formation of the nucleus. This process is accelerated in the presence of crowders due to an excluded volume effect (much as is the case with increasing concentration). Crowding is much less effective in accelerating aggregation in the case of aggregation prone conformations. In this case, the rate-limiting step lies in the addition of monomers at the extremities of the fibrils, and this can be hindered by the presence of crowding agents. Research remains to be done on elucidating the kinetics of aggregation, the nature of the oligomeric species and the end-products of aggregation in the presence of different types of crowding agents. A second emerging area of research lies in studying the interaction of aggregating peptides with surfaces, and in particular with lipid membranes. Experiments suggest that surfaces can nucleate the aggregation of peptides, or that peptides can insert into membranes and form cytotoxic pores [117–120], or that peptide aggregates deposited on the membrane can damage the membrane [121], the last two factors possibly playing an important role in amyloid-related diseases [122]. Much work remains to be done in modeling protein–membrane interactions, in large part because

coarse-grained models of lipid membranes [123,124] are not as well developed as the corresponding models for proteins. Caflisch and coworkers studied aggregation on the surface of coarse-grained lipid vesicles and showed that highly amyloidogenic peptides aggregate to form fibrils on the surface of the vesicle, damaging its structure and promoting leakage [55,56]. Leakage was found to be due to the growing aggregates and not to the mature fibrils. Peptides are seen to adsorb on the vesicle surface and aggregate via an ordered templating mechanism. Related simulation of aggregation on surfaces was performed by Auer and coworkers [63•] who investigated the aggregation of their tube model on spherical nanoparticles. Their simulations revealed a condensation-ordering mechanism, reminiscent of what was observed in the bulk that was independent of particle size or hydrophobicity. In a first step, peptides adsorb on the particle and form small disordered oligomers on the particle surface, followed by a second step in which they rearrange their structure to form ordered β-sheets. The rates of aggregation are increased in the presence of a nanoparticle due to an increase in local concentration (as was seen in the simulations of Caflisch). The nanoparticle acts as a seed, effectively removing the nucleation barrier (and associated lag time).

Conclusion

The coarse-grained models described in the preceding paragraphs have provided considerable insight into the mechanisms of aggregation and have unified many of the disparate observations from experiment. They have shown that the intrinsic β-sheet (aggregation) propensity of the peptide plays a key role in determining the pathways for fibril formation and the nature of the prefibrillar oligomers. Fibril formation was seen to proceed either through the formation of amorphous oligomeric species, or directly from ordered aggregate states. The simulations supported a 'nucleation-growth' mechanism, and shed light into the nature of the nucleus as well as into the mechanisms of fibril elongation. Fibril growth was seen to proceed by lateral growth (through the addition of preformed layers, or through the templated growth of disordered species) or by longitudinal growth, primarily through monomer addition, either via a dock-lock mech-

Figure 2

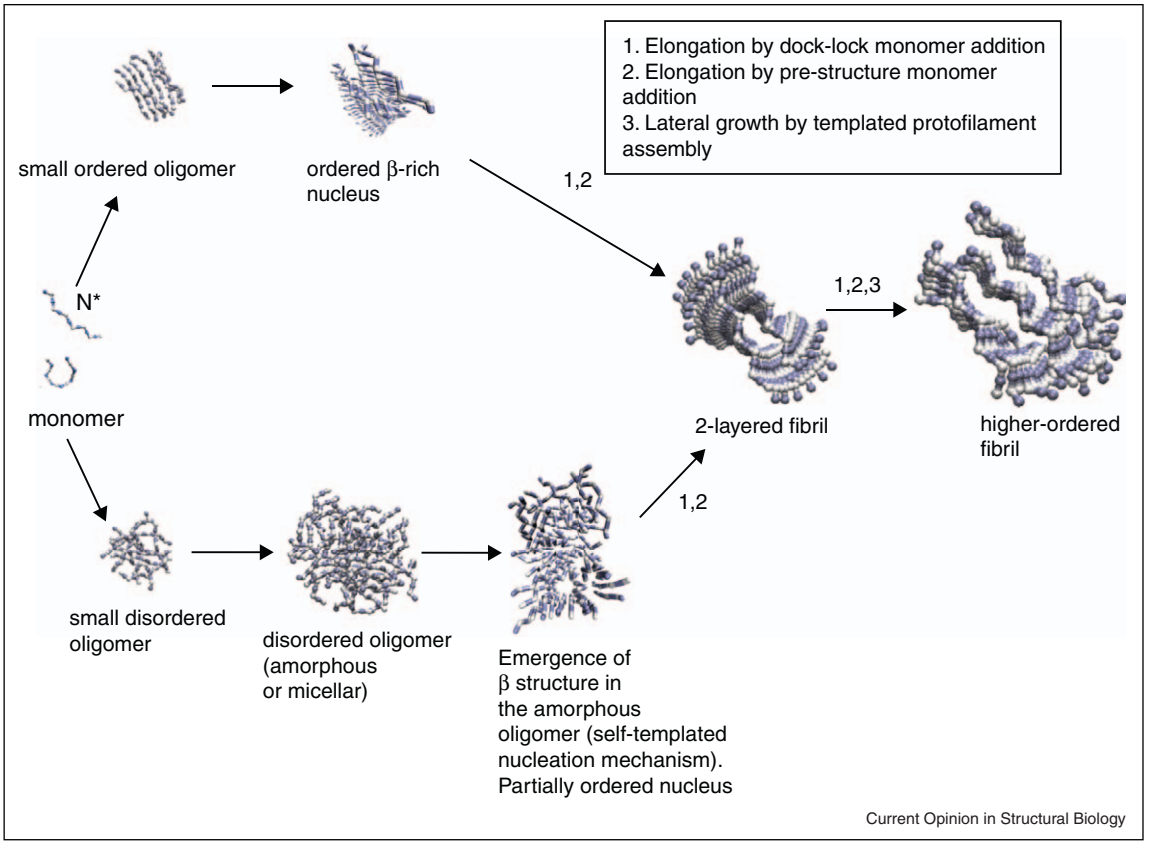

A unified aggregation scenario emerging from the coarse-grained studies. Aggregation can proceed via multiple pathways. The monomer can populate a number of conformations, including an amyloid-competent N* conformation. The upper pathway corresponds to fibril formation via the formation of ordered aggregates, while the lower pathway corresponds to fibril formation via disordered aggregates. Fibril elongation can occur by three mechanisms: (1) elongation by dock-lock monomer addition; (2) elongation by prestructured monomer addition; (3) lateral growth by templated protofilament assembly. Fibril elongation dominates in the final stages of fibril growth. Adapted from [59••,54••].

anism, or via a mechanism in which the monomer first prestructured to a fibril-competent conformation before assembly. It is remarkable that the coarse-grained models that differ significantly in terms of resolution, yield such consistent mechanisms for fibril formation. The generic nature of the mechanisms that emerge from the coarse-grained simulations highlights the commonalities between aggregating peptides. They explain why so many peptides, with different sequences and native folds, form aggregates that are structurally similar, from oligomers that can bind the same antibodies, to the final cross-β fibril morphology.

A summary of the main fibrillization pathways and mechanisms is shown in Figure 2.

Acknowledgements

Support from the NSF (MCB 0642086, DMR05-20415 and LRAC MCA 05S027), the NIH (AG027818) and the David and Lucile Packard Foundation are gratefully acknowledged. We thank Giovanni Bellesia, Amedeo Pellarin, Stefan Auer, Mai Suan Li, and Dave Thirumalai for helpful comments and for providing figures.

References and recommended reading

Papers of particular interest, published within the period of review, have been highlighted as:

- • of special interest
- •• of outstanding interest

1. Selkoe DJ: **Cell biology of protein misfolding: the examples of Alzheimer's and Parkinson's diseases**. *Nat Cell Biol* 2004, **6**:1054-1061.
2. Chiti F, Dobson CM: **Protein misfolding, functional amyloid, and human disease**. *Annu Rev Biochem* 2006, **75**:333-366.
3. Fandrich M, Forge V, Buder K, Kittler M, Dobson CM, Diekmann S: **Myoglobin forms amyloid fibrils by association of unfolded polypeptide segments**. *Proc Natl Acad Sci U S A* 2003, **100**:15463-15468.
4. Bucciantini M, Giannoni E, Chiti F, Baroni F, Formigli L, Zurdo J, Taddei N, Ramponi G, Dobson CM, Stefani M: **Inherent toxicity of aggregates implies a common mechanism for protein misfolding diseases**. *Nature* 2002, **416**:507-511.
5. Fowler DM, Koulov AV, Balch WE, Kelly JW: **Functional amyloid — from bacteria to humans**. *Trends Biochem Sci* 2007, **32**:217-224.
6. Zhang S: **Fabrication of novel biomaterials through molecular self-assembly**. *Nat Biotechnol* 2003, **21**:1171-1178.
7. Sunde M, Blake C: **The structure of amyloid fibrils by electron microscopy and X-ray diffraction**. *Adv Protein Chem* 1997, **50**:123-159.
8. Luhrs T, Ritter C, Adrian M, Riek-Loher D, Bohrmann B, Doeli H, Schubert D, Riek R: **3D structure of Alzheimer's amyloid-β(1–42) fibrils**. *Proc Natl Acad Sci U S A* 2005, **102**:17342-17347.
9. Petkova AT, Ishii Y, Balbach JJ, Antzutkin ON, Leapman RD, Delaglio F, Tycko R: **A structural model for Alzheimer's Abeta-amyloid fibrils based on experimental constraints from solid state NMR**. *Proc Natl Acad Sci U S A* 2002, **99**:16742-16747.
10. Luca S, Yau WM, Leapman R, Tycko R: **Peptide conformation and supramolecular organization in amylin fibrils: constraints from solid-state NMR**. *Biochemistry (Mosc)* 2007, **46**:13505-13522.
11. Serpell LC, Sunde M, Benson MD, Tennent GA, Pepys MB, Fraser PE: **The protofilament substructure of amyloid fibrils**. *J Mol Biol* 2000, **300**:1033-1039.
12. Serpell LC, Sunde M, Blake CCF: **The molecular basis of amyloidosis**. *Cell Mol Life Sci* 1997, **53**:871-887.
13. Sunde M, Serpell LC, Bartlam M, Fraser PE, Pepys MB, Blake CCF: **Common core structure of amyloid fibrils by synchrotron X-ray diffraction**. *J Mol Biol* 1997, **273**:729-739.
14. Tycko R: **Molecular structure of amyloid fibrils: insights from solid-state NMR**. *Q Rev Biophys* 2006, **39**:1-55.
15. Harper JD, Lansbury PT Jr: **Models of amyloid seeding in Alzheimer's disease and scrapie: mechanistic truths and physiological consequences of the time-dependent solubility of amyloid proteins**. *Annu Rev Biochem* 1997, **66**:385-407.
16. Padrick SB, Miranker AD: **Islet amyloid: phase partitioning and secondary nucleation are central to the mechanism of fibrillogenesis**. *Biochemistry (Mosc)* 2002, **41**:4694-4703.
17. Lambert MP: **Diffusible, nonfibrillar ligands derived from Aβ1–42 are potent central nervous system neurotoxins**. *Proc Natl Acad Sci U S A* 1998, **95**:6448-6453.
18. Walsh DM, Lomakin A, Benedek GB, Condron MM, Teplow DB: **Amyloid β-protein fibrillogenesis — detection of a protofibrillar intermediate**. *J Biol Chem* 1997, **272**:22364-22372.
19. Shankar GM, Li SM, Mehta TH, Garcia-Munoz A, Shepardson NE, Smith I, Brett FM, Farrell MA, Rowan MJ, Lemere CA *et al.*: **Amyloid-β protein dimers isolated directly from Alzheimer's brains impair synaptic plasticity and memory**. *Nat Med* 2008, **14**:837-842.
20. Carulla NI, Zhou M, Arimon M, Gairi M, Giralt E, Robinson CV, Dobson CM: **Experimental characterization of disordered and ordered aggregates populated during the process of amyloid fibril formation**. *Proc Natl Acad Sci U S A* 2009, **106**:7828-7833.
21. Haass C, Selkoe DJ: **Soluble protein oligomers in neurodegeneration: lessons from the Alzheimer's amyloid Aβ-peptide**. *Nat Rev Mol Cell Biol* 2007, **8**:101-112.
22. Goldsbury C, Kistler J, Aebi U, Arvinte T, Cooper GJS: **Watching amyloid fibrils grow by time-lapse atomic force microscopy**. *J Mol Biol* 1999, **285**:33-39.
23. Marek P, Abedini A, Song BB, Kanungo M, Johnson ME, Gupta R, Zaman W, Wong SS, Raleigh DP: **Aromatic interactions are not required for amyloid fibril formation by islet amyloid polypeptide but do influence the rate of fibril formation and fibril morphology**. *Biochemistry (Mosc)* 2007, **46**:3255-3261.
24. Kayed R, Bernhagen J, Greenfield N, Sweimeh K, Brunner H, Voelter W, Kapurniotu A: **Conformational transitions of islet amyloid polypeptide (IAPP) in amyloid formation in vitro**. *J Mol Biol* 1999, **287**:781-796.
25. Abedini A, Raleigh DP: **A role for helical intermediates in amyloid formation by natively unfolded polypeptides?** *Phys Biol* 2009, **6**:015005.
26. Williamson JA, Miranker AD: **Direct detection of transient α-helical states in islet amyloid polypeptide**. *Protein Sci* 2007, **16**:110-117.
27. Shim SH, Gupta R, Ling YL, Strasfeld DB, Raleigh DP, Zanni MT: **Two-dimensional IR spectroscopy and isotope labeling defines the pathway of amyloid formation with residue-specific resolution**. *Proc Natl Acad Sci U S A* 2009, **106**:6614-6619.
28. Bernstein SL, Dupuis NF, Lazo ND, Wyttenbach T, Condron MM, Bitan G, Teplow DB, Shea J-E, Ruotolo BT, Robinson CV *et al.*: **Amyloid-β protein oligomerization and the importance of tetramers and dodecamers in the aetiology of Alzheimer's disease**. *Nat Chem* 2009, **1**:326-331.
29. Dupuis NF, Wu C, Shea J-E, Bowers MT: **Human islet amyloid polypeptide monomers form ordered β-hairpins: a possible direct amyloidogenic precursor**. *J Am Chem Soc* 2009, **191**:18283-18292.
30. Baumketner A, Bernstein SL, Wyttenbach T, Bitan G, Teplow DB, Bowers MT, Shea J-E: **Amyloid β-protein monomer structure: a computational and experimental study**. *Protein Sci* 2006, **15**:420-428.

31. Thirumalai D, Klimov DK, Dima RI: **Emerging ideas on the molecular basis of protein and peptide aggregation**. *Curr Opin Struct Biol* 2003, **13**:146-159.

32. Tarus B, Straub JE, Thirumalai D: **Dynamics of Asp23-Lys28 salt-bridge formation in Aβ10–35 monomers**. *J Am Chem Soc* 2006, **128**:16159-16168.

33. Nam HB, Kouza M, Zung H, Li MS: **Relationship between population of the fibril-prone conformation in the monomeric state and oligomer formation times of peptides: insights from all-atom simulations**. *J Chem Phys* 2010, **132**:165104-165110.

34. Straub JE, Thirumalai D: **Principles governing oligomer formation in amyloidogenic peptides**. *Curr Opin Struct Biol* 2010, **20**:187-195.

35. Ma B, Nussinov R: **Simulations as analytical tools to understand protein aggregation and predict amyloid conformation**. *Curr Opin Chem Biol* 2006, **10**:445-452.

36. Jang S, Shin S: **Computational study on the structural diversity of amyloid β peptide (Aβ(10–35)) oligomers**. *J Phys Chem B* 2008, **112**:3479-3484.

37. Masman MF, Eisel ULM, Csizmadia IG, Penke B, Enriz RD, Marrink SJ, Luiten PGM: **In silico study of full-length amyloid β (1–42) tri- and penta-oligomers in solution**. *J Phys Chem B* 2009, **113**:11710-11719.

38. Reddy G, Straub JE, Thirumalai D: **Influence of preformed Asp23-Lys28 salt bridge on the conformational fluctuations of monomers and dimers of Aβ peptides with implications for rates of fibril formation**. *J Phys Chem B* 2009, **113**: 1162-1172.

39. Sgourakis NG, Yan Y, McCallum SA, Wang C, Garcia AE: **The Alzheimer's peptides Aβ40 and 42 adopt distinct conformations in water: a combined MD/NMR study**. *J Mol Biol* 2007, **368**:1448-1457.

40. Tarus B, Straub JE, Thirumalai D: **Probing the initial stage of aggregation of the Aβ10–35 protein: assessing the propensity for peptide dimerization**. *J Mol Biol* 2005, **345**:1141-1156.

41. Miller Y, Ma B, Nussinov R: **Polymorphism of Alzheimer's Aβ17–42(p3) oligomers: the importance of the turn location and its conformation**. *Biophys J* 2009, **97**:1168-1177.

42. Wu C, Bowers MT, Shea J-E: **Molecular structures of quiescently-grown and brain-derived polymorphic fibrils of the Alzheimer amyloid Aβ 9–40 peptide: a comparison to agitated fibrils**. *PLoS Comp Biol* 2010, **6**:e1000693.

43. Buchete NV, Hummer G: **Structure and dynamics of parallel β-sheets, hydrophobic core, and loops in Alzheimer's Aβ fibrils**. *Biophys J* 2007, **92**:3032-3039.

44. Patro SY, Przybycien TM: **Simulations of reversible protein aggregate and crystal structure**. *Biophys J* 1996, **70**:2888-2902.

45. • Zhang J, Muthukumar M: **Simulations of nucleation and elongation of amyloid fibrils**. *J Chem Phys* 2009, **130**:035102.
The authors perform Monte Carlo simulations of the assembly of identical cuboid units (see Figure 1a), where each cuboid represents an extended peptide, a folded peptide, or a small oligomer. An important result from their simulations is that nucleation is directly linked to the semi two-dimensional nature of fibrils, with a highly cooperative barrier for forming a two-layered β-sheet seed responsible for the nucleation lag phase.

46. Dima RI, Thirumalai D: **Exploring protein aggregation and self-propagation using lattice models: phase diagram and kinetics**. *Protein Sci* 2002, **11**:1036-1049.

47. •• Li MS, Klimov DK, Straub JE, Thirumalai D: **Probing the mechanisms of fibril formation using lattice models**. *J Chem Phys* 2008, **129**:175101.
The authors use a lattice model (see Figure 1b) to study the aggregation of small peptides. An important outcome of their work is the identification of an 'Ostwald ripening' mechanism for fibril growth that they showed quantitatively follows the Lifshitz–Syazov growth law.

48. Cellmer T, Bratko D, Prausnitz JM, Blanch H: **Protein-folding landscapes in multichain systems**. *Proc Natl Acad Sci U S A* 2005, **102**:11692-11697.

49. Fawzi NL, Okabe Y, Yap E-H, Head-Gordon T: **Determining the critical nucleus and mechanism of fibril elongation of the Alzheimer's Aβ1–40 peptide**. *J Mol Biol* 2007, **365**:535-550.

50. • Li MS, Co NT, Reddy G, Hu C-K, Straub JE, Thirumalai D: **Factors governing fibrillogenesis of polypeptide chains revealed by lattice models**. *Phys Rev Lett* 2010, **105**:218101.
This study reveals the role of N* (fibril-prone monomeric conformations) in determining the rates of fibril formation and the propensity of sequences to form fibrils.

51. Garai K, Sahoo B, Sengupta P, Maiti S: **Quasihomogeneous nucleation of amyloid β yields numerical bounds for the critical radius, the surface tension, and the free energy barrier for nucleus formation**. *J Chem Phys* 2008, **128**:045102.

52. Bellesia G, Shea J-E: **Self-assembly of β-sheet forming peptides into chiral fibrillar aggregates**. *J Chem Phys* 2007, **126**:245104.

53. • Bellesia G, Shea J-E: **Diversity of kinetic pathways in amyloid fibril formation**. *J Chem Phys* 2009, **131**:111102.
This paper explores the effect of β-sheet propensity in governing the pathways for fibril formation. The number of pathways leading to fibril formation is seen to increase with decreasing β-sheet propensity. Peptides with low β-sheet propensity aggregate via disordered intermediates. Peptides with intermediate β-sheet propensity assemble either through the formation of amorphous aggregates, β-barrel (nonfibrillar) aggregates or directly from monomers through ordered β-sheet aggregates. Peptides with high β-sheet propensity formed fibrils uniquely via ordered aggregates.

54. •• Bellesia G, Shea J-E: **Effect of β-sheet propensity on peptide aggregation**. *J Chem Phys* 2009, **130**:145103.
This paper introduces a dihedral parameter that governs the flexibility (or β-sheet propensity) of their coarse-grained model. Their simulations reveal that peptides with low-β sheet propensity populate a greater diversity of oligomeric states (including amorphous aggregates and β-barrel structures) than peptides with high β-sheet propensity.

55. Friedman R, Pellarin R, Caflisch A: **Soluble protofibrils as metastable intermediates in simulations of amyloid fibril degradation induced by lipid vesicles**. *J Phys Chem Lett* 2010, **1**:471-474.

56. Friedman R, Pellarin R, Caflisch A: **Amyloid aggregation on lipid bilayers and its impact on membrane permeability**. *J Mol Biol* 2009, **387**:407-415.

57. • Magno A, Caflisch A, Pellarin R: **Crowding effects on amyloid aggregation kinetics**. *J Phys Chem Lett* 2010, **1**:3027-3032.
This is one of the first studies to investigate the role of crowding agents on the kinetics of fibril formation. Their work reveals that the effect of crowding differs for peptides with high and low aggregation propensities.

58. Pellarin R, Caflisch A: **Interpreting the aggregation kinetics of amyloid peptides**. *J Mol Biol* 2006, **360**:882-892.

59. •• Pellarin R, Guarnera E, Caflisch A: **Pathways and intermediates of amyloid fibril formation**. *J Mol Biol* 2007, **374**:917-924.
This paper examines the aggregation process of peptides with different levels of aggregation propensity. An important outcome of this work is that the pathways and nature of the intermediates are dictated by aggregation propensity. Peptides with low aggregation propensity are seen to aggregate via a micellar intermediate state, while peptides with high aggregation propensities aggregate from β-rich monomers without forming micelles.

60. Pellarin R, Schuetz P, Guarnera E, Caflisch A: **Amyloid fibril polymorphism is under kinetic control**. *J Am Chem Soc* 2010, **132**:14960-14970.

61. •• Auer S, Dobson CM, Vendruscolo M, Maritan A: **Self-templated nucleation in peptide and protein aggregation**. *Phys Rev Lett* 2008, **101**:258101.
Using the 'tube' model (Figure 1b), the authors identify a self-templated nucleation mechanism that explains the transition from disordered assemblies to fibrillar structure. Their simulations show that the peptides can rearrange their structures within the disordered assemblies into β-rich fibrillar structures, the surfaces of which serve as templates for further growth.

62. Auer S, Meersman F, Dobson CM, Vendruscolo M: **A generic mechanism of emergence of amyloid protofilaments from disordered oligomeric aggregates**. *PLoS Comp Biol* 2008, **4**:e1000222.

63. Auer S, Trovato A, Vendruscolo M: **A condensation-ordering mechanism in nanoparticle-catalyzed peptide aggregation**. *PLoS Comp Biol* 2009, **5**:e1000458.
This is one of the first studies to look at how surfaces can catalyze the aggregation of peptides to form fibrils. Their simulations reveal that aggregation on surfaces is a two-step process, involving the formation of disordered aggregates that assemble on the surface and then restructure to form β-rich fibrils.

64. Auer S, Kashchiev D: **Phase diagram of α-helical and β-sheet forming peptides**. *Phys Rev Lett* 2010, **104**:168105.

65. Urbanc B, Betnel M, Cruz L, Bitan G, Teplow DB: **Elucidation of amyloid β-protein oligomerization mechanisms: discrete molecular dynamics study**. *J Am Chem Soc* 2010, **132**:4266-4280.

66. Gobbi M, Colombo L, Morbin M, Mazzoleni G, Accardo E, Vanoni M, Del Favero E, Cantu L, Kirschner DA, Manzoni C *et al.*: **Gerstmann–Straeussler–Scheinker disease amyloid protein polymerizes according to the 'dock-and-lock' model**. *J Biol Chem* 2006, **281**:843-849.

67. Nguyen HD, Hall CK: **Molecular dynamics simulations of spontaneous fibril formation by random-coil peptides**. *Proc Natl Acad Sci U S A* 2004, **101**:16180-16185.

68. Urbanc B, Cruz L, Ding F, Sammond D, Khare S, Buldyrev SV, Stanley HE, Dokholyan NV: **Molecular dynamics simulation of amyloid β dimer formation**. *Biophys J* 2004, **87**:2310-2321.

69. Dima RI, Settanni G, Micheletti C, Banavar JR, Maritan A: **Extraction of interaction potentials between amino acids from native protein structures**. *J Chem Phys* 2000, **112**:9151-9166.

70. Heo M, Kim S, Moon EJ, Cheon M, Chung K, Chang I: **Perceptron learning of pairwise contact energies for proteins incorporating the amino acid environment**. *Phys Rev E* 2005, **72**:1-9.

71. Jernigan RL, Bahar I: **Structure-derived potentials and protein simulations**. *Curr Opin Struct Biol* 1996, **6**:195-209.

72. Meller J, Wagner M, Elber R: **Maximum feasibility guideline in the design and analysis of protein folding potentials**. *J Comput Chem* 2002, **23**:111-118.

73. Mirny LA, Shakhnovich EI: **How to derive a protein folding potential? A new approach to an old problem**. *J Mol Biol* 1996, **264**:1164-1179.

74. Park B, Levitt M: **Energy functions that discriminate X-ray and near-native folds from well-constructed decoys**. *J Mol Biol* 1996, **258**:367-392.

75. Sippl MJ: **Knowledge-based potentials for proteins**. *Curr Opin Struct Biol* 1995, **5**:229-235.

76. Thomas PD, Dill KA: **An iterative method for extracting energy-like quantities from protein structures**. *Proc Natl Acad Sci U S A* 1996, **93**:11628-11633.

77. Bellesia G, Jewett AI, Shea J-E: **Sequence periodicity and secondary structure propensity in model proteins**. *Protein Sci* 2010, **19**:141-154.

78. Lomakin A, Chung DS, Benedek GB, Kirschner DA, Teplow DB: **On the nucleation and growth of amyloid Aβ protein fibrils: detection of nuclei and quantitation of rate constants**. *Proc Natl Acad Sci U S A* 1996, **93**:1125-1129.

79. Chen SM, Ferrone FA, Wetzel R: **Huntington's disease age-of-onset linked to polyglutamine aggregation nucleation**. *Proc Natl Acad Sci U S A* 2002, **99**:11884-11889.

80. Liang Y, Lynn DG, Berland KM: **Direct observation of nucleation and growth in amyloid self-assembly**. *J Am Chem Soc* 2010, **132**:6306-6308.

81. Kashchiev D, Auer S: **Nucleation of amyloid fibrils**. *J Chem Phys* 2010, **132**:215101.

82. Auer S, Dobson CM, Vendruscolo M: **Characterization of the nucleation barriers for protein aggregation and amyloid formation**. *Hfsp J* 2007, **1**:137-146.

83. Serio TR, Cashikar AG, Kowal AS, Sawicki GJ, Moslehi JJ, Serpell L, Arnsdorf MF, Lindquist SL: **Nucleated conformational conversion and the replication of conformational information by a prion determinant**. *Science* 2000, **289**:1317-1321.

84. Cheon M, Chang I, Hall CK: **Extending the PRIME model for protein aggregation to all 20 amino acids**. *Proteins Struct Funct Bioinf* 2010, **78**:2950-2960.

85. Nguyen HD, Hall CK: **Spontaneous fibril formation by polyalanines; discontinuous molecular dynamics simulations**. *J Am Chem Soc* 2006, **128**:1890-1901.

86. Urbanc B, Cruz L, Yun S, Buldyrev SV, Bitan G, Teplow DB, Stanley HE: **In silico study of amyloid β-protein folding and oligomerization**. *Proc Natl Acad Sci U S A* 2004, **101**: 17345-17350.

87. Bitan G, Kirkitadze MD, Lomakin A, Vollers SS, Benedek GB, Teplow DB: **Amyloid β-protein (Aβ) assembly: Aβ40 and Aβ42 oligomerize through distinct pathways**. *Proc Natl Acad Sci U S A* 2003, **100**:330-335.

88. Melchor JP, McVoy L, Van Nostrand WE: **Charge alterations of E22 enhance the pathogenic properties of the amyloid β-protein**. *J Neurochem* 2000, **74**:2209-2212.

89. Van Nostrand WE, Melchor JP, Cho HS, Greenberg SM, Rebeck GW: **Pathogenic effects of D23N Iowa mutant amyloid β-protein**. *J Biol Chem* 2001, **276**:32860-32866.

90. Crescenzi O, Tomaselli S, Guerrini R, Salvadori S, D'Ursi AM, Temussi PA, Picone D: **Solution structure of the Alzheimer amyloid β-peptide (1–42) in an apolar microenvironment — similarity with a virus fusion domain**. *Eur J Biochem* 2002, **269**:5642-5648.

91. Eakin CM, Attenello FJ, Morgan CJ, Miranker AD: **Oligomeric assembly of native-like precursors precedes amyloid formation by β2 microglobulin**. *Biochemistry (Mosc)* 2004, **43**:7808-7815.

92. Teplow DB, Lazo ND, Bitan G, Bernstein S, Wyttenbach T, Bowers MT, Baumketner A, Shea J-E, Urbanc B, Cruz L *et al.*: **Elucidating amyloid β-protein folding and assembly: a multidisciplinary approach**. *Acc Chem Res* 2006, **39**:635-645.

93. Gazit E: **Self-assembled peptide nanostructures: the design of molecular building blocks and their technological utilization**. *Chem Soc Rev* 2007, **36**:1263-1269.

94. Tjernberg L, Hosia W, Bark N, Thyberg J, Johansson J: **Charge attraction and β propensity are necessary for amyloid fibril formation from tetrapeptides**. *J Biol Chem* 2002, **277**: 43243-43246.

95. Balbirnie M, Grothe R, Eisenberg DS: **An amyloid-forming peptide from the yeast prion Sup35 reveals a dehydrated β-sheet structure for amyloid**. *Proc Natl Acad Sci U S A* 2001, **98**:2375-2380.

96. Baumketner A, Shea JE: **Free energy landscapes for amyloidogenic tetrapeptides dimerization**. *Biophys J* 2005, **89**:1493-1503.

97. Bellesia G, Shea J-E: **What determines the structure and stability of KFFE monomers, dimers, and protofibrils?** *Biophys J* 2009, **96**:875-886.

98. Reddy AS, Wang L, Lin YS, Ling Y, Chopra M, Zanni MT, Skinner JL, De Pablo JJ: **Solution structures of rat amylin peptide: simulation, theory, and experiment**. *Biophys J* 2010, **98**:443-451.

99. Reddy AS, Wang L, Singh S, Ling Y, Buchanan L, Zanni MT, Skinner JL, De Pablo JJ: **Stable and metastable states of human amylin in solution**. *Biophys J* 2010, **99**:2208-2216.

100. Nilsberth C, Westlind-Danielsson A, Eckman CB, Condron MM, Axelman K, Forsell C, Stenh C, Luthman J, Teplow DB, Younkin SG *et al.*: **The 'Arctic' APP mutation (E693G) causes Alzheimer's disease by enhanced Aβ protofibril formation**. *Nat Neurosci* 2001, **4**:887-893.

101. Lashuel HA: **Mixtures of wild-type and a pathogenic (E22G) form of Aβ40 in vitro accumulate protofibrils, including amyloid pores**. *J Mol Biol* 2003, **332**:795-808.

102. Teplow DB: **Structural and kinetic features of amyloid β-protein fibrillogenesis**. *Amyloid J Protein Fold Disord* 1998, **5**:121-142.

103. Williams AD, Sega M, Chen ML, Kheterpal I, Geva M, Berthelier V, Kaleta DT, Cook KD, Wetzel R: **Structural properties of Aβ protofibrils stabilized by a small molecule**. *Proc Natl Acad Sci U S A* 2005, **102**:7115-7120.

104. Kheterpal I, Chen M, Cook KD, Wetzel R: **Structural differences in Aβ amyloid protofibrils and fibrils mapped by hydrogen exchange — mass spectrometry with on-line proteolytic fragmentation**. *J Mol Biol* 2006, **361**:785-795.

105. Harper JD, Wong SS, Lieber CM, Lansbury PT Jr: **Assembly of β-amyloid protofibrils: an in vitro model for a possible early event in Alzheimer's disease**. *Biochemistry (Mosc)* 1999, **38**: 8972-8980.

106. Walsh DM, Hartley DM, Kusumoto Y, Fezoui Y, Condron MM, Lomakin A, Benedek GB, Selkoe DJ, Teplow DB: **Amyloid β-protein fibrillogenesis. Structure and biological activity of protofibrillar intermediates**. *J Biol Chem* 1999, **274**: 25945-25952.

107. Nichols MR, Moss MA, Reed DK, Lin W-L, Mukhopadhyay R, Hoh JH, Rosenberry TL: **Growth of β-Amyloid(1–40) protofibrils by monomer elongation and lateral association. Characterization of distinct products by light scattering and atomic force microscopy**. *Biochemistry (Mosc)* 2002, **41**: 6115-6127.

108. Yagi H, Ban T, Morigaki K, Naiki H, Goto Y: **Visualization and classification of amyloid β supramolecular assemblies**. *Biochemistry (Mosc)* 2007, **46**:15009-15017.

109. Massi F, Straub JE: **Energy landscape theory for Alzheimer's amyloid β-peptide fibril elongation**. *Proteins Struct Funct Genet* 2001, **42**:217-229.

110. Straub JE, Thirumalai D: **Towards a molecular theory of early and late events in monomer to amyloid fibril**. *Annu Rev Phys Chem* 2011, **62**:437-463.

111. Tarus B, Straub JE, Thirumalai D: **Probing the initial stage of aggregation of the Aβ(10–35)-protein: Assessing the propensity for peptide dimerization**. *J Mol Biol* 2005, **345**: 1141-1156.

112. Esler WP, Stimson ER, Ghilardi JR, Lu YA, Felix AM, Vinters HV, Mantyh PW, Lee JP, Maggio JE: **Point substitution in the central hydrophobic cluster of a human β-amyloid congener disrupts peptide folding and abolishes plaque competence**. *Biochemistry (Mosc)* 1996, **35**: 13914-13921.

113. Esler WP, Stimson ER, Jennings JM, Vinters HV, Ghilardi JR, Lee JP, Mantyh PW, Maggio JE: **Alzheimer's disease amyloid propagation by a template-dependent dock-lock mechanism**. *Biochemistry (Mosc)* 2000, **39**:6288-6295.

114. Green JD, Goldsbury C, Kistler J, Cooper GJS, Aebi U: **Human Amylin oligomer growth and fibril elongation define two distinct phases in amyloid formation**. *J Biol Chem* 2004, **279**:12206-12212.

115. Sciarretta KL, Gordon DJ, Petkova AT, Tycko R, Meredith SC: **Aβ40-lactam (D23/K28) models a conformation highly favorable for nucleation of amyloid**. *Biochemistry (Mosc)* 2005, **44**:6003-6014.

116. Paravastu AK, Qahwash I, Leapman RD, Meredith SC, Tycko R: **Seeded growth of β-amyloid fibrils from Alzheimer's brain-derived fibrils produces a distinct fibril structure**. *Proc Natl Acad Sci U S A* 2009, **106**:7443-7448.

117. Knight JD, Miranker AD: **Phospholipid catalysis of diabetic amyloid assembly**. *J Mol Biol* 2004, **341**:1175-1187.

118. Choo-Smith L-PÄ, Garzon-Rodriguez W, Glabe CG, Surewicz WK: **Acceleration of amyloid fibril formation by specific binding of Aβ(1–40) peptide to ganglioside-containing membrane vesicles**. *J Biol Chem* 1997, **272**:22987-22990.

119. Jang H, Arce FT, Ramachandran S, Capone R, Azimova R, Kagan BL, Nussinov R, Lal R: **Truncated β-amyloid peptide channels provide an alternative mechanism for Alzheimer's disease and Down syndrome**. *Proc Natl Acad Sci U S A* 2010, **107**:6538-6543.

120. Arispe N: **Architecture of the Alzheimer's AßP ion channel pore**. *J Membr Biol* 2004, **197**:33-48.

121. Ambroggio EE, Kim DH, Separovic F, Barrow CJ, Barnham KJ, Bagatolli LA, Fidelio GD: **Surface behavior and lipid interaction of Alzheimer β-amyloid peptide 1–42: a membrane-disrupting peptide**. *Biophys J* 2005, **88**:2706-2713.

122. Stefani M: **Biochemical and biophysical features of both oligomer/fibril and cell membrane in amyloid cytotoxicity**. *FEBS J* 2010, **277**:4602-4613.

123. Brannigan G, Philips PF, Brown FLH: **Flexible lipid bilayers in implicit solvent**. *Phys Rev E* 2005, **72**:011915.

124. Cooke IR, Deserno M: **Solvent-free model for self-assembling fluid bilayer membranes: stabilization of the fluid phase based on broad attractive tail potentials**. *J Chem Phys* 2005, **123**:224710.

125. Wei GH, Song W, Derreumaux P, Mousseau N: **Self-assembly of amyloid-forming peptides by molecular dynamics simulations**. *Front Biosci* 2008, **13**:5681-5692.

126. Irback A, Mohanty S: **PROFASI: a Monte Carlo simulation package for protein folding and aggregation**. *J Comput Chem* 2006, **27**:1548-1555.